KI REPORTS
KIReports.org
TRANSLATIONAL RESEARCH

Rapid On-Site Histopathological Analysis of Kidney Biopsy With Dynamic Full-Field Optical Coherence Tomography

Léa Zuccarelli[1], Quentin Bernard[2], Georges Tarris[3], Laurent Martin[3], Mathilde Funes de la Vega[3], Amélie Jacq[1], Jean-Michel Rebibou[1], Claire Tinel[1], Claude Boccara[4], Olivier Thouvenin[4], Jean-Marie Chassot[4], Marion Rabant[5], Julien Zuber[6,7], Christophe Legendre[6,7], Jean-Pierre Quenot[8,9,10], Marie-Noëlle Peraldi[6,7], Lucile Amrouche[6,7], Anne Scemla[6], Nathalie Chavarot[6,7], Dany Anglicheau[6,7], Mathieu Legendre[1,11] and Thomas Maldiney[8,12]

[1]Department of Nephrology, CHU Dijon, Dijon, France; [2]Department of Nephrology, William Morey General Hospital, Chalon-sur-Saône, France; [3]Department of Pathology, Dijon University Hospital, Dijon, France; [4]Department of Medical and Biological Imaging, Institut Langevin, ESPCI Paris, PSL University, CNRS, Paris, France; [5]Pathology department, Necker-Enfants Malades Hospital, Paris, France; [6]Faculty of Medicine, Université Paris-Cité, Paris, France; [7]Department of Kidney and Metabolic Diseases, Transplantation and Clinical Immunology, Necker Hospital, AP-HP, Paris, France; [8]Lipness Team, Institut national de la santé et de la recherche médicale (INSERM) Research Centre Lipides, Nutrition, Cancer – Unité mixte de recherche (LNC-UMR) 1231, University of Burgundy, Dijon, France; [9]CIC1432, Clinical Epidemiology Unit, Institut national de la santé et de la recherche médicale (INSERM), Dijon, France; [10]Department of Intensive Care Medicine, Dijon Bourgogne University Hospital, Dijon, France; [11]LEAD-CNRS, UMR 5022, Université de Bourgogne, Dijon, France; and [12]Department of Intensive Care Medicine, William Morey General Hospital, Chalon-sur-Saône, France

Introduction: Kidney histology preparation requires a multistep process that is usually responsible for delayed results. This study introduces dynamic full-field optical coherence tomography (D-FF-OCT) as a label-free alternative to overcome the limitations of traditional histopathology for on-site kidney pathology assessment.

Methods: Two patient cohorts were considered, with a total of 31 patients included in the study; one cohort involved patients requiring biopsy of transplant kidney, and the other involved patients requiring biopsy of native kidney. The clinical and biological data were prospectively collected. Histopathological analysis of kidney biopsies was conducted using both conventional stains and dynamic D-FF-OCT imaging.

Results: D-FF-OCT enabled the recognition of most kidney structures. The results showed a significant correlation between this technology and conventional stains for the evaluation of both interstitial fibrosis (IF) ($r = 0.61$, $P < 0.001$) and tubular atrophy (TA) ($r = 0.60$, $P < 0.001$). Although many lesions could be identified such as interstitial inflammation, acute tubular necrosis, glomerular crescents, and vascular intimal thickening; other recognitions such as glomerular membranous deposits, vascular amyloidosis, and peritubular capillaritis will require confirmation in larger cohorts.

Conclusion: This study demonstrates the potential of D-FF-OCT imaging for on-site analysis of kidney biopsies, providing rapid and high-resolution images without extensive sample preparation.

Kidney Int Rep (2025) **10,** 1529–1537; https://doi.org/10.1016/j.ekir.2025.01.047
KEYWORDS: dynamic contrast; dynamic full-field optical coherence tomography; kidney pathology

Chronic kidney disease affects more than 840 million individuals and is one of the leading causes of death worldwide.[1] The etiological diagnosis and prognosis of chronic kidney disease mostly rely on histopathological analysis of both native and transplanted kidney biopsies. Nevertheless, kidney histopathology can suffer from several limitations, notably an incompressible preparation time, which could delay the results and subsequent administration of the appropriate treatment.[2] Therefore, minimizing the delay between kidney biopsy and subsequent diagnosis would require the development of an alternative

Correspondence: Thomas Maldiney, Centre Hospitalier William Morey, 4 rue du Capitaine Drillien, Chalon-sur-Saône, France. E-mail: thomas.maldiney@ch-chalon71.fr

Received 1 October 2024; revised 27 January 2025; accepted 31 January 2025; published online 6 February 2025

technological solution to allow rapid histopathological analysis without extensive preparation of the tissue sample.

Full-field optical coherence tomography (FF-OCT) is a high-resolution variant of OCT, also known as the optical equivalent of an ultrasound scanner.[3] It exploits the principle of interferometric detection at low coherence to quantify the light propagation time in scattering tissues. FF-OCT enables the measurement of the light naturally backscattered by the many optical interfaces found in biological tissues and provides optical sectioning by selecting the time of flight of these photons. FF-OCT captures the average number of photons backscattered at a given depth with high isotropic resolution of $1 \times 1 \times 1\ \mu m^3$. Overall, FF-OCT is a label-free optical microscopy technique that is particularly efficient for capturing the organization of the extracellular matrix in a large field of view.[4]

D-FF-OCT uses the same experimental device as FF-OCT; however, image production relies on the analysis of backscattered photon fluctuations over time at a given depth, instead of taking the average number as in FF-OCT. As a result, D-FF-OCT cannot only detect living cells in explants, but it can also provide additional information regarding the metabolic or stress-induced activity of the cells that control cellular active transport (Supplementary Table S1). Combining the ability of FF-OCT to detect extracellular matrix organization with the ability of D-FF-OCT to detect cells and nuclei offers a label-free alternative to conventional histopathological staining while providing similar information.[4-6] Compared with other dynamic OCT,[7] D-FF-OCT shows superior transverse resolution and can access subcellular details.

Manu Jain *et al*. previously studied the ability of FF-OCT, to evaluate *ex vivo* kidney tissue from nephrectomy samples within minutes. Through this preliminary work, they identified some components of the cortical area and differentiated neoplastic from non-neoplastic kidney tissue, without extensive preparation of tissue samples.[8] However, their technology was unable to reveal living cells within these kidney specimens. To circumvent this critical limitation hampering the future of this technology for histopathological analysis of living tissue, D-FF-OCT was developed as an updated setup with the ability to return additional information regarding subcellular metabolic contrasts[5] and subsequent metabolic activity of living cells.[9] To the best of our knowledge, D-FF-OCT has never been applied to kidney pathology.[7] Because this modality enables a first step label-free and nondestructive fast imaging before tissue fixation, coloration, and comparative analysis with standard histology, we hypothesized that D-FF-OCT may serve for bedside instant evaluation of biopsy quality and provide rapid on-site information about the structures and lesions in native and transplant kidney pathology.

METHODS

Population

The patients included participated in 2 protocols; one involving kidney transplant recipients from Necker Hospital between November 2021 and April 2022 (DIVAT cohort, NCT02900040), and the other involving patients who underwent native kidney biopsy at William Morey Hospital between November 2022 and May 2023 (NEPHROCT cohort, NCT05728216). In French, DIVAT stands for "Données Informatisées et VAlidées en Transplantation" (computerized and validated data in transplantation). It relates to a database which allows the collection of medical records for kidney transplantations. A total of 8 centers participate in France, with the aim of allowing epidemiological research studies in kidney transplant recipients, focusing on both clinical outcomes and therapeutic strategies. In addition, the NEPHROCT cohort stands for NEPHROpathological analysis of renal biopsies with D-FF-OCT, with the objective of comparing D-FF-OCT with conventional histopathological findings for the diagnosis of either acute kidney injury or chronic kidney disease in routine practice.

Patients had to be aged 18 years or older and not subjected to any legal protection measure. Clinical and biological data on the day of the biopsy were prospectively collected, including age, gender, history of diabetes, hypertension, causal nephropathy, serum creatinine level, and proteinuria. Estimation of the glomerular filtration rate was calculated using the Chronic Kidney Disease-Epidemiology formula.[10]

The local Ethics Committee and Dijon University Hospital Delegate for Clinical Research and Innovation approved the study. Included patients gave oral approval for the study protocol.

D-FF-OCT Imaging and Image Analysis

D-FF-OCT images were obtained using a D-FF-OCT apparatus (Light-CT Scanner, LLTech - Aquyre Biosciences, Paris, France) on biopsies before fixation (Figure 1).[11] Samples were oriented to match the histological protocols. Illumination was performed with either a conventional halogen light source with a short temporal coherence length (DIVAT cohort) or a light-emitting diode source centered at a wavelength of 565 nm (NEPHROCT cohort).[12] Owing to technical constraints, D-FF-OCT biopsies from the DIVAT cohort

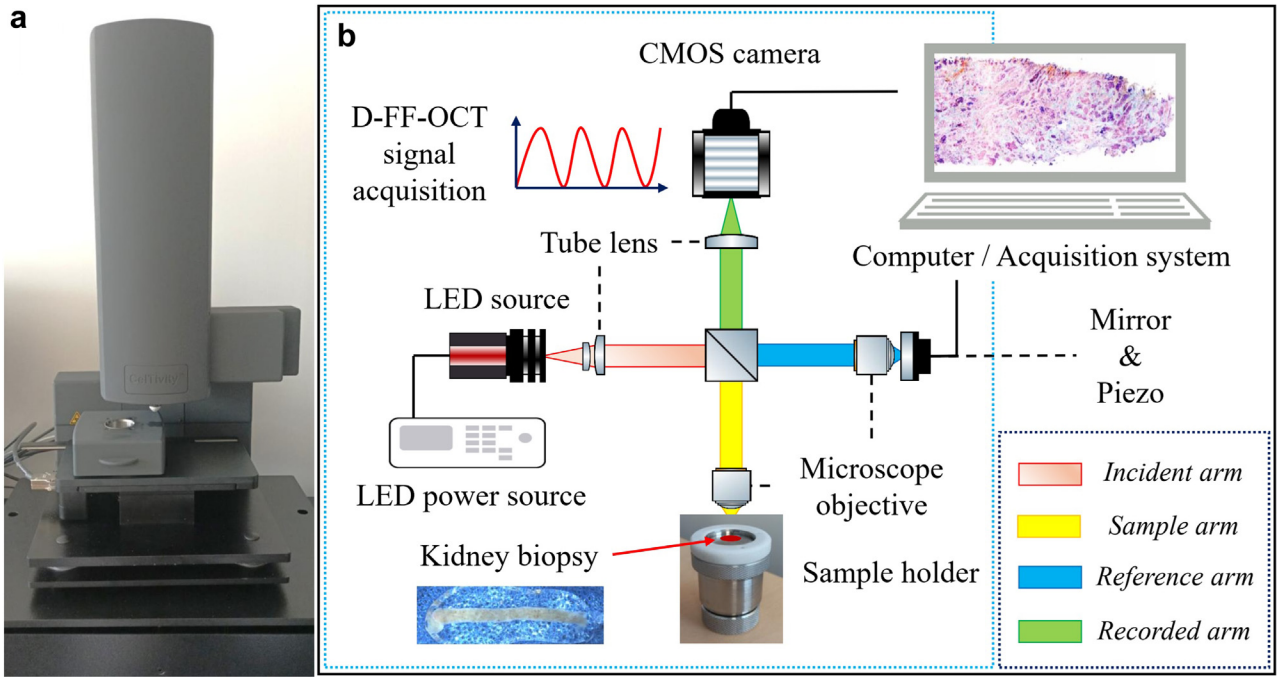

Figure 1. Example of a native kidney biopsy sample acquisition. D-FF-OCT (a) apparatus and (b) its mechanics. A white light emitting diode source illuminates a beam splitter (incident arm) that separates the light into a reference arm and a sample arm. The interference signal created from the reunion of both arms will be captured by a camera (recorded arm) and translated into an image. In dynamic contrast images, colors from each pixel are obtained by analyzing the time series of each pixel using a fast Fourier transform program. The spectrum obtained is then divided into 3 parts associated to the 3 colors of the composite RGB image, associating fast movements to red colors, moderate movements to green colors, and slow movements to blue colors. D-FF-OCT, dynamic full field optical coherence tomography; LED, light emitting diode.

were sent for immunofluorescent analysis, whereas biopsies from the NEPHROCT cohort were sent for optical microscopy analysis.

FF-OCT images correspond to the average number of photons backscattered from each pixel and from the same depth in the sample, thus correspond to a single value, represented as a monochrome image. D-FF-OCT images correspond to the temporal fluctuations of this number, which is a complex and multiparametric signal. For easier visualization, we calculated 3 metrics, which we combined to form an RGB image.[13] In practice, D-FF-OCT images generated by the CelTivity are pseudo-colored RGB images, where each color channel is built on the Fourier-domain analysis of the signal fluctuations (Supplementary Figure S1A and B) integrated on 3 different frequency ranges. The low (0–0.6 Hz), medium (0.6–5.4 Hz), and high (5.4–25 Hz) frequencies were color-coded into blue, green, and red, respectively, and combined to form the D-FF-OCT image (Supplementary Figure S1C).

A series of 50 D-FF-OCT slices (1266 × 1266 μm^2) were recorded with 1 µm spacing in depth and reconstructed using ImageJ 1.52o software (National Institutes of Health, Bethesda, MD). All images were assessed to identify the corresponding depth observed under light microscopy, because D-FF-OCT provided only superficial information up to a depth of 50 µm. Images were processed using ImageJ 1.52o software. The ImageJ "z-stack" function is available in this standard version of 1.52o installation and served to combine images as sums of 3 µm spacing in depth to match local pathological standards. Dynamic contrast images were posttreated with color inversion to improve readability. Kidney biopsies were treated with formaldehyde-based fixative agents right after D-FF-OCT analysis to provide the best tissue preparation for conventional histopathological staining and analysis.

Histological Analysis

The biopsy samples were formalin-fixed and paraffin-embedded, then cut into 3 µm–thick sections before conventional staining, including hematoxylin, eosin, and saffron; Masson's Blue Trichrome stain, Periodic Acid Schiff stain, and silver stain. The slides were then digitized using a Nanozoomer 2.0 HT (Hamamatsu, Japan). Visual analyses were blindly performed for OCT in comparison with all conventional stains by 2 kidney pathologists with a French degree in kidney pathology. When the data evaluated were on a continuous scale or semicontinuous with 5% increments, the resulting integer from the mean of the assessments was retained. For the comparison with OCT, the average value between kidney pathologists' assessments was utilized. The assessment of transplant

lesions was based on the classification from both Banff 2019 and 2022 Kidney Meeting Reports.[14,15] For data derived from the Banff classification, in cases of discrepancy between pathologists, a consensus value was reached after a review. An adequate biopsy was defined as a biopsy with more than 8 nonglobally sclerotic glomeruli. For the DIVAT cohort biopsies, the glomerular count was performed on the frozen hematoxylin eosin saffron–stained section, whereas the assessment of fibrosis and atrophy scores was conducted on conventional stains.

Statistical Analysis

Quantitative data were expressed as median and interquartile range and semiquantitative data as numbers and percentages. The correlation between 2 quantitative variables was calculated using the Spearman test. Wilcoxon's paired test was used to compare 2 quantitative variables. Kappa coefficients were used as measures of interrater reliability. A kappa score < 0.40 is poor, 0.40–0.59 is moderate, 0.60–0.79 is substantial; and 0.80 is outstanding. Receiver operating characteristics curves were constructed for prediction by the tool of pathologists' scores. The Youden's test was used to determine the threshold with best specificity and sensitivity on receiver operating characteristics curves. Statistical analysis was performed using GraphPad PRISM 6.01 software (GraphPad Software, La Jolla, CA) and IBM SPSS 23 software (IBM, Chicago, IL).

RESULTS

Population Characteristics

A total of 31 patients were included, 16 patients had a transplant biopsy and 15 had a native kidney biopsy. One patient was excluded because of technical issues in D-FF-OCT acquisition. Kidney diseases, Banff scores, and population baseline characteristics are shown in Tables 1 and 2. Mean age at biopsy was 58 (43–69) years, 39% were women, and most patients (63%) had a history of hypertension. Among native biopsies, the most frequent cause of kidney failure was minimal change disease. The median serum creatinine at biopsy was 2.0 (1.2–2.6) mg/dl, and the mean estimated glomerular filtration rate was 32 (23–65) ml/min per 1.73 m^2 (Table 1). The most frequent Banff lesions in transplant kidney biopsies were IF ci $\geq$ 1 (56%), TA ct $\geq$ 1 (56%), vascular fibrous intimal thickening cv $\geq$ 1 (63%), and arteriolar hyalinosis ah $\geq$ 1 (63%).

D-FF-OCT Imaging of Normal Kidney Structures

The mean global acquisition and processing time with D-FF-OCT was approximately 30 minutes per biopsy, given the scheme described in Figure 1. Almost instant screening of the whole biopsy with FF-OCT was accessible in less than a minute. D-FF-OCT imaging allowed the identification of the capsular, medullary, and cortical areas, as depicted in Figure 2 and Supplementary Figure S2. First, a macro image of the kidney biopsy inside the sample holder was recorded before any D-FF-OCT acquisition (Figure 2a and b). Then, FF-OCT images were recorded and reconstructed to display the whole biopsy (Figure 2c). The FF-OCT signal appeared as a grayscale image with the most intense signal (close to white) depicting the capsular area; IF; and the outermost arterial tunica, the tunica adventitia. A less intense and darker FF-OCT signal (close to pale gray) was identified within the tubular area, glomeruli, or both the inner and middle layers of arteries (Figure 2c). In contrast, the D-FF-OCT signal from Figure 3d (direct D-FF-OCT) and Figure 3e (inverted D-FF-OCT) enlightened the most cellular parts of the whole kidney biopsy, mainly revealing inflammatory, tubular, and glomerular cells. In addition, as shown in the comparison with hematoxylin and eosin stains displayed in Figure 3f, the inverted D-FF-OCT signal returns an overall aspect of the biopsy relatively close to the one observed with conventional histopathology (Masson's Trichrome stain).

A more precise overview of glomeruli, arteries tunicae, tubular, and interstitial areas is shown in Figure 3. Notably, the capillary tuft was distinguishable from the Bowman's space following further analysis of the glomerulus with D-FF-OCT (Figure 3a–d). Linked to the limited depth analyzed with D-FF-OCT (50 μm), the number of detected nonglobally sclerotic glomeruli tended to be lower than that with optical microscopy. A median of 13 (6–21) glomeruli per biopsy in optical microscopy and 5 (2–11) in D-FF-OCT were counted ($P < 0.001$). The area under the receiver operating characteristics curve to predict an adequate biopsy with the glomeruli in D-FF-OCT was 0.90 (95% confidence interval [0.80–0.99], $P < 0.001$). Detecting at least 5 glomeruli on D-FF-OCT predicted an adequate biopsy with a sensitivity of 71% and a specificity of 90%. Tubular and interstitial areas are shown in Figure 3e–h. The FF-OCT image unveils the most intense signal within the interstitial area (Figure 3e) when D-FF-OCT dynamic images mostly reveal the tubular cells from this area of the biopsy (Figure 3f and g). The comparison of Figures 3g and 3h highlights a closer correspondence between the inverted D-FF-OCT signal and the conventional colors of the Masson's trichrome stain for the identification of tubules. A similar description can be adapted for the visualization of arteries (Figure 3i–l). Notably, Figure 3i shows how the vascular tunics appear properly differentiated by the FF-OCT signal, with the most intense values for the tunica adventitia or the internal elastic laminae, and a

Table 1. Description of the study population

Characteristics	All patients ($N = 31$)	Transplant biopsies ($n = 16$, DIVAT cohort)	Native biopsies ($n = 15$, NEPHROCT cohort)
Median age at biopsy (yrs, IQR)	58 (43–69)	48 (43–64)	61 (38–73)
Gender (*n*, %)			
Female	12 (39)	10 (63)	1 (7)
Male	19 (61)	6 (37)	14 (93)
History of hypertension	20 (63)	12 (75)	8 (53)
Diabetes	4 (13)	2 (13)	2 (13)
Median serum creatinine at biopsy (mg/dl)	2.0 (1.2–2.6)	1.9 (1.3–2.6)	2.0 (1.2–3.2)
Median eGFR at biopsy (ml/min per 1,73 m^2)	32 (23–65)	35 (23–57)	31 (15–66)
Median proteinuria at biopsy (g/g, IQ)	1.3 (0.2–4.0)	0.7 (0.1–3.6)	2.4 (1.0–4.3)
Histological diagnosis (*n*, %)			
Normal	8 (26)	8 (50)	
Antibody mediated chronic rejection	1 (3)	1 (6)	
Chronic active T cell-mediated rejection	1 (3)	1 (6)	
IgA nephropathy	2 (6)	1 (6)	1 (7)
Thrombotic microangiopathy	1 (3)	1 (6)	
Hemosiderosis	1 (3)	1 (6)	
Focal segmental glomerulosclerosis	1 (3)	1 (6)	
Minimal changes disease	3 (10)		3 (20)
B cell lymphoma infiltration	1 (3)		1 (7)
IgA vasculitis	1 (3)		1 (7)
Nephrosclerosis	2 (6)		2 (13)
Membranous nephropathy	2 (6)		2 (13)
Acute tubular necrosis	2 (6)		2 (13)
Randall disease	1 (3)		1 (7)
Vascular AL amyloidosis	1 (3)		1 (7)
Malignant hypertension	1 (3)		1 (7)
Unknown	1 (3)		1 (7)

eGFR, estimated glomerular filtration rate.

more greyish contrast within the tunica media. In contrast, a switch to the dynamic mode of D-FF-OCT mostly enlightens both endothelial and smooth muscle cells (Figure 3j and 3k), when compared with the Periodic Acid Schiff stain (Figure 3l).

As shown in Figure 4a and b, the degree of IF/TA was not significantly different between conventional or standard stains and D-FF-OCT (median of 15% [10%–40%] and 18% [10%–40%], respectively, $P = 0.818$). The D-FF-OCT percentages of IF and TA were well-correlated with those of classical stains ($r = 0.61$, $P < 0.001$, and $r = 0.60$, $P < 0.001$, respectively). In addition, as shown in Figure 4c, the area under the receiver operating characteristics curve for the prediction of IF/TA >25% was 0.88 (95% confidence interval [0.75–0.99], $P = 0.001$). We conducted an interpathologist comparison for the degree of IF/TA, with a kappa between 2 pathologists on conventional histology measured at 0.84 for a global IF/TA > 25% ($P < 0.0001$), and a kappa between 2 pathologists on D-FF-OCT measured at 0.60 for IF > 25% ($P = 0.001$) and 0.58 for TA > 25% ($P = 0.001$).

Table 2. Banff lesions in transplant kidney biopsies

Banff lesions (*n*, %)	Classical stain ($n = 16$)
Interstitial inflammation *i* ≥ 1	0 (0)
Tubulitis *t* ≥ 1	3 (19)
Intimal arteritis *v* ≥ 1	2 (13)
Glomerulitis *g* ≥ 1	2 (13)
Peritubular capillaritis *ptc* ≥ 1	5 (31)
C4d ≥ 1	2 (13)
Interstitial fibrosis *ci* ≥ 1	9 (56)
Tubular atrophy *ct* ≥ 1	9 (56)
Vascular fibrous intimal thickening*cv* ≥ 1	10 (63)
Glomerular basement double contour *cg* ≥ 1	1 (6)
Mesangial matrix expansion *mm* ≥ 1	1 (6)
Arteriolar hyalinosis *ah* ≥ 1	10 (63)
Hyaline arteriolar thickening *aah* ≥ 1	0 (0)
Total inflammation *ti* ≥ 1	2 (13)
Inflammation in the area of interstitial fibrosis and tubular atrophy *i-IFTA* ≥ 1	3 (19)

The occurrence "classical stain" refers to either hematoxylin and eosin stain, periodic acid schiff stain, Masson's blue trichrome stain, or silver stain.

Lesions Assessment

Several lesions were identified with D-FF-OCT. Among them, we could distinguish glomerular crescents, acute tubular necrosis, a pseudo-thyroid aspect of renal tubuli and red blood cell casts, arterial fibrointimal thickening (Supplementary Figure S3), a subcapsular infiltrate of a chronic lymphocytic leukemia, interstitial inflammatory areas, and expansion of glomerular mesangial matrix (Supplementary Figure S4). Two patients had membranous nephropathy, and 1 patient had vascular amyloidosis, which were not detected with D-FF-OCT;

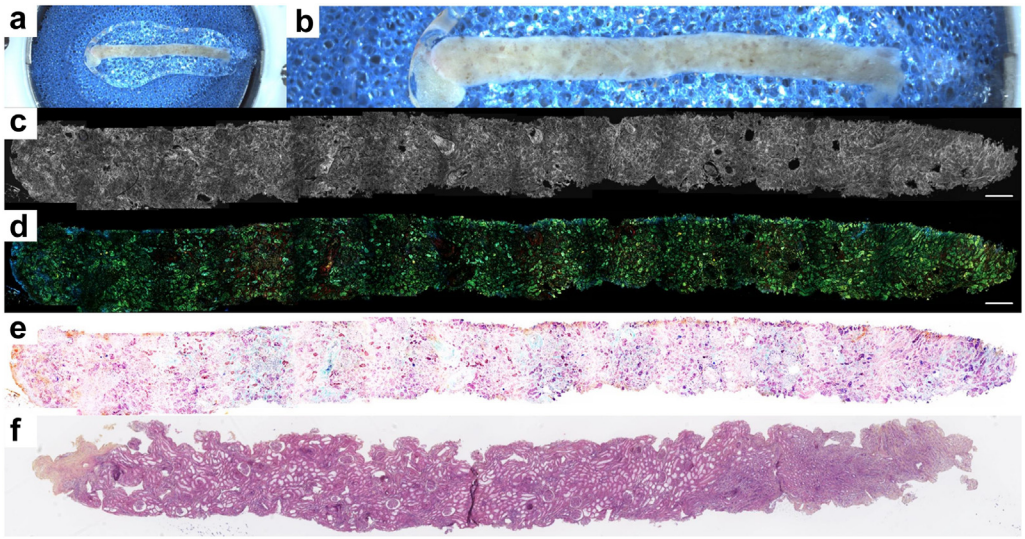

Figure 2. D-FF-OCT imaging of a whole kidney biopsy. Kidney biopsy sample on (a, b) the apparatus, (c) FF-OCT, (d) D-FF-OCT, (e) reversed D-FF-OCT, and (f) hematoxylin and eosin stain. The whole biopsy is 1.5 cm long. D-FF-OCT, dynamic full field optical coherence tomography. Scale bar represents 500 μm.

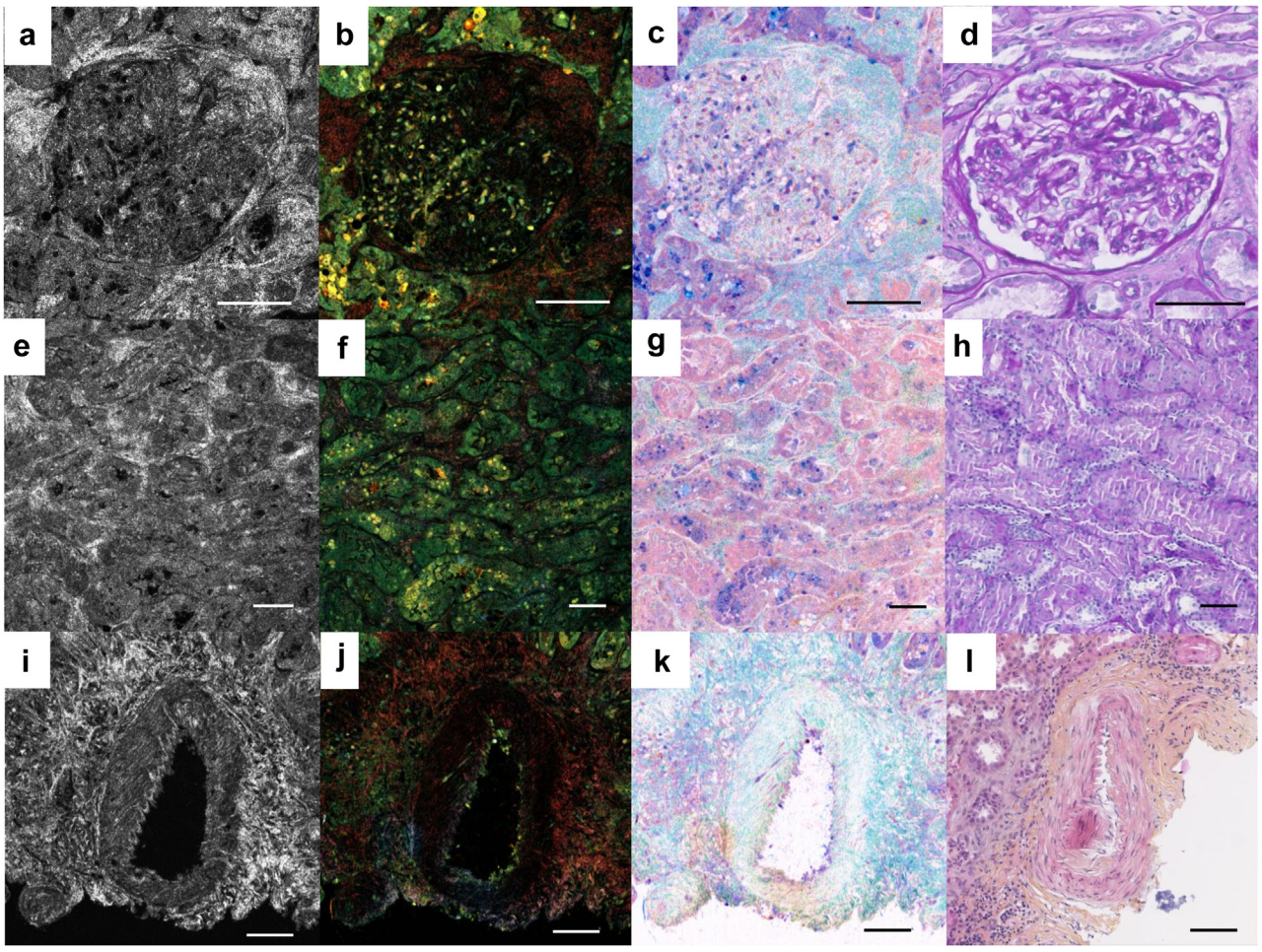

Figure 3. D-FF-OCT and corresponding usual staining of elementary kidney structures. Glomerulus with minimal change disease is shown in (a) FF-OCT, (b) D-FF-OCT, (c) reversed D-FF-OCT, and (d) periodic acid Schiff stain. Interstitial tissue from the corticomedullary junction area is shown in (e) FF-OCT, (f) D-FF-OCT, (g) reversed D-FF-OCT, and (h) periodic acid Schiff stain. A healthy artery is shown in (i) FF-OCT, (j) D-FF-OCT, (k) reversed D-FF-OCT, and (l) hematoxylin and eosin stain. Scale bar represents 100 μm. AT, tubular atrophy; D-FF-OCT, dynamic full field optical coherence tomography; IF, interstitial fibrosis.

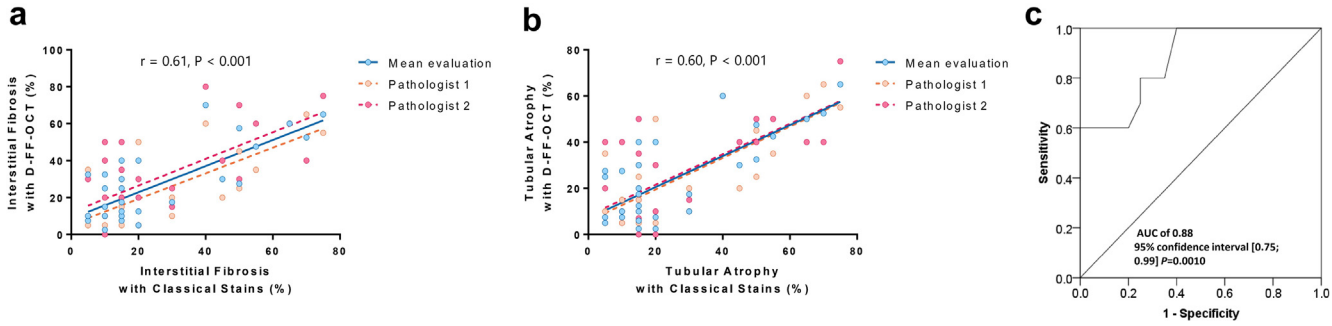

Figure 4. Association between D-FF-OCT and conventional stains evaluated for IF and AT. (a) Association for IF, (b) association for AT, and (c) ROC-curves to predict an IF/TA. D-FF-OCT percentage of IF and TA were well-correlated with those of classical stains ($r = 0.61$, $P < 0.001$, and $r = 0.60$, $P < 0.001$, respectively). The area under the ROC curve for prediction of IF/TA > 25% was 0.88 (95% confidence interval [0.75–0.99], $P = 0.001$). AT, tubular atrophy; D-FF-OCT, dynamic full field optical coherence tomography; IF, interstitial fibrosis; ROC, receiver operating characteristic.

peritubular capillaritis and hemosiderosis were not discernible, and arteriolar hyalinosis evaluation was limited in the present cohorts (Supplementary Figure S4).

DISCUSSION

This study presents the first results of label-free D-FF-OCT imaging in native and transplant kidney biopsies. D-FF-OCT provides immediate images with high resolution of different structures of the kidneys without tissue processing. It demonstrates the ability of such technology to rapidly return precious information about both quality and preliminary histopathological analysis of kidney biopsy, within a few minutes, providing not only direct identification of the capsular, medullary, and cortical areas, but also multiple lesion assessment and semiquantitative analysis of IF and TA. Despite some promising results related to this unprecedented application of D-FF-OCT for instant histopathological analysis of kidney biopsy, the present study suffers from potential limitations that can hamper immediate transposition to clinical routine practice.

First, the images were not perfectly super imposable between D-FF-OCT and histology. Because the biopsy is a rotating cylinder, it is rather complicated to maintain the specimen in a fixed position. Indeed, D-FF-OCT detects fluctuations caused by the transport of small and dimmer organelles, and it is more crucial to have a good signal-to-noise ratio (SNR) as for FF-OCT. As in any other imaging modality, signal-to-noise ratio decreases with imaging depth because of tissue light scattering. Histology only looks at 5 μm slices, confocal microscopy can image up to approximately the same depth of 50 μm, whereas FF-OCT or biphoton microscopy could image further in samples down to 200 μm to 300 μm. Such penetration depths strongly depend on sample scattering properties and on the wavelength. For instance, in near infrared D-FF-OCT, imaging up to 400 μm in retinal organoids was demonstrated.[16] In the case of kidney tissue imaging, D-FF-OCT imaging deeper than 50 μm is responsible for significant light scattering and absorption, both responsible for a poor signal-to-noise ratio. Consequently, the cortical area per analyzed section will be smaller than in conventional histology, limiting, for example, the number of glomeruli analyzed per section. The more superficial the analyzed layer, the smaller the analyzed surface area. Thus, this maximum depth is a significant limitation in interpreting the results and would require further correlation with standard histopathological images to allow proper determination of quantitative parameters (IF, TA, transplant lesion evaluation based on conventional Banff classification for allograft pathology).

The assessment of DIVAT cohort biopsies was performed on frozen sections, thereby limiting comparability for transplant lesion evaluation on the basis of conventional Banff Classification for Allograft Pathology.[14,15,17] In addition, the halogen light source yielded lower-quality images, suggesting systematic use of the light-emitting diode source for future experiments. Precise imaging of the glomerulus and several other specific lesions that are not accessible in the present cohort with D-FF-OCT will require further spectral analysis of the dynamic contrast signal from each cell.

Using FF-OCT, Jain *et al.*[8] have been able to identify some components of nonneoplastic kidney tissues on nephrectomy specimens. Such an addition of dynamic acquisitions and focus on kidney biopsies seemed to provide a complementary representation of the kidney histology, with a potential direct application in nephrology clinical practice. Because D-FF-OCT evaluation of glomerular crescents and IF as well as most of tubular and vascular lesions seemed to be accurate, one could imagine using D-FF-OCT for rapid diagnosis of

crescentic glomerulonephritis or for the quality assessment of grafts in preimplantation biopsies. When compared with light microscopy, the number of glomeruli detected in D-FF-OCT was lower because D-FF-OCT is limited to the external layer of the biopsy sample. Villarreal *et al.*[18] recently investigated confocal microscopy in a fusion mode alongside hematoxylin and eosin staining. Like our study, they obtained images of lesions, such as acute tubular necrosis and IF changes; however, the acquired images exhibited a lower resolution, and a lower depth of imaging. D-FF-OCT may however help in confirming kidney cortical sampling, ensuring an adequate number of glomeruli, therefore quickly guide as to whether there is a need for another sample.[19]

It should be noted that none of the transplant biopsies displayed significant inflammation outside of fibrotic areas. This is likely because of the small size of our transplant cohort (16 biopsies), and the fact that some were protocol biopsies. As a result, this limits the generalizability of our findings, particularly concerning T cell–mediated rejection analysis. In addition, 2 native kidney biopsies demonstrated significant inflammatory infiltrates, including one case of lymphoma infiltration.

This study provides promising D-FF-OCT results with immediate, less processing, noninvasive (i.e., preserving RNA and DNA for further molecular biology analysis), high-quality, 2-dimensional images of kidney biopsies. Regarding native kidney biopsies, D-FF-OCT could provide an easy, convenient, and quick way to confirm the quality of native kidney tissue. For donor evaluation transplant biopsies, a quick D-FF-OCT–based evaluation of the degree of chronic injury and chronic vascular disease could be of precious help to provide a complementary diagnostic tool for the identification of the proper type of organ dysfunction, with the aim of better guiding treatment and future graft prognosis for the clinician. In addition, such technology could contribute to the identification of new extended donor criteria based on pretransplant histological evaluation of kidney transplants, thereby opening alternatives for a better evaluation of poor outcome-associated kidneys and their possible discard before transplantation.

DISCLOSURE

All the authors declared no competing interests.

ACKNOWLEDGMENTS

The authors sincerely thank Cathy Sezeur and Nathalie Dullier Taillefumier for their help with slide digitalization using the Nanozoomer 2.0 HT, along with all volunteers from the Association pour la Recherche Médicale en Saône-et-Loire (ARMSL) for the research funding.

Funding

This work was supported by the Association pour la Recherche Médicale en Saône-et-Loire (ARMSL, https://www.armsl.org/). The findings and conclusions in this report are those of the authors and do not necessarily represent the official position of the funding organization.

DATA AVAILABILITY STATEMENT

All data from this study are included in this article. Further inquiries can be directed to the corresponding author.

AUTHOR CONTRIBUTIONS

LM, CB, J-MR, CT, DA, ML, and TM designed the study, conducted the experiments, and performed the experimental work. LZ, ML, and TM wrote the manuscript. LZ, QB, GT, MFV, AJ, CB, OT, JMC, MR, JZ, CL, MNP, LA, AS, NC, DA, ML and TM performed the experimental works. LZ, QB, GT, LM, MFdlV, AJ, J-MR, CT, CB, OT, J-MC, MR, JZ, CL, J-PQ, M-NP, LA, AS, NC, DA, ML, and TM contributed to the revision of the manuscript. MR, DA, ML, and TM supervised the project. All the authors contributed to the article and approved the submitted version.

SUPPLEMENTARY MATERIAL

Supplementary File (PDF)

Figure S1. Schematic principle of D-FF-OCT signal acquisition and transformation into pseudo-colored RGB image, example of a glomerulus.

Figure S2. D-FF-OCT and corresponding usual staining of different areas of native kidney biopsies.

Figure S3. D-FF-OCT and corresponding usual stains of pathological structures in native kidney biopsies.

Figure S4. D-FF-OCT and corresponding usual stains of pathological structures in transplant kidney biopsies.

Table S1. Comparison of Full-Field Optical Coherence Tomography (FF-OCT) and Dynamic FF-OCT (D-FF-OCT) imaging modalities.

STROBE Statement.

REFERENCES

1. Kovesdy CP. Epidemiology of chronic kidney disease: An update 2022. *Kidney Int Suppl.* 2022;12:7–11. https://doi.org/10.1016/j.kisu.2021.11.003
2. Schnuelle P. Renal biopsy for diagnosis in kidney disease: Indication, technique, and safety. *JCM.* 2023;12:6424. https://doi.org/10.3390/jcm12196424
3. Dubois A, Vabre L, Boccara AC, Beaurepaire E. High-resolution full-field optical coherence tomography with a Linnik microscope. *Appl Opt.* 2002;41:805–812. https://doi.org/10.1364/AO.41.000805
4. Thouvenin O, Apelian C, Nahas A, Fink M, Boccara C. Full-field optical coherence tomography as a diagnosis tool:

Recent progress with multimodal imaging. *Appl Sci*. 2017;7:236. https://doi.org/10.3390/app7030236

5. Apelian C, Harms F, Thouvenin O, Boccara AC. Dynamic full field optical coherence tomography: Subcellular metabolic contrast revealed in tissues by interferometric signals temporal analysis. *Biomed Opt Express*. 2016;7:1511–1524. https://doi.org/10.1364/BOE.7.001511
6. Scholler J, Mandache D, Mathieu MC, et al. Automatic diagnosis and classification of breast surgical samples with dynamic full-field OCT and machine learning. *J Med Imaging (Bellingham)*. 2023;10:034504. https://doi.org/10.1117/1.JMI.10.3.034504
7. Ren C, Hao S, Wang F, et al. Dynamic contrast optical coherence tomography (DyC-OCT) for label-free live cell imaging. *Commun Biol*. 2024;7:278. https://doi.org/10.1038/s42003-024-05973-5
8. Jain M, Robinson BD, Salamoon B, Thouvenin O, Boccara C, Mukherjee S. Rapid evaluation of fresh ex vivo kidney tissue with full-field optical coherence tomography. *J Pathol Inform*. 2015;6:53. https://doi.org/10.4103/2153-3539.166014
9. Groux K, Verschueren A, Nanteau C, et al. Dynamic full-field optical coherence tomography allows live imaging of retinal pigment epithelium stress model. *Commun Biol*. 2022;5:575. https://doi.org/10.1038/s42003-022-03479-6
10. Levey AS, Stevens LA, Schmid CH, et al. A new equation to estimate glomerular filtration rate. *Ann Intern Med*. 2009;150:604–612. https://doi.org/10.7326/0003-4819-150-9-200905050-00006
11. Ghouali W, Grieve K, Bellefqih S, et al. Full-field optical coherence tomography of human donor and pathological corneas. *Curr Eye Res*. 2015;40:526–534. https://doi.org/10.3109/02713683.2014.935444
12. Wang L, Fu R, Xu C, Xu M. Methods and applications of full-filed optical coherence tomography: A review. *J Biomed Opt*. 2022;27:050901. https://doi.org/10.1117/1.JBO.27.5.050901
13. Apelian C, Gastaud C, Boccara AC. Extracting relevant information for cancer diagnosis from dynamic full field OCT through image processing and learning. In: Fujimoto JG, Izatt JA, Tuchin VV, eds. *Optical Coherence Tomography and Coherence Domain Optical Methods in Biomedicine XXI*. Proceedings of SPIE; 2017:10053H. https://doi.org/10.1117/12.2254824
14. Loupy A, Haas M, Roufosse C, et al. The Banff 2019 Kidney Meeting Report (I): Updates on and clarification of criteria for T cell– and antibody-mediated rejection. *Am J Transplant*. 2020;20:2318–2331. https://doi.org/10.1111/ajt.15898
15. Naesens M, Roufosse C, Haas M, et al. The Banff 2022 Kidney Meeting Report: Reappraisal of microvascular inflammation and the role of biopsy-based transcript diagnostics. *Am J Transplant*. 2024;24:338–349. https://doi.org/10.1016/j.ajt.2023.10.016
16. Monfort T, Azzollini S, Brogard J, et al. Dynamic full-field optical coherence tomography module adapted to commercial microscopes allows longitudinal in vitro cell culture study. *Commun Biol*. 2023;6:992. https://doi.org/10.1038/s42003-023-05378-w
17. Loupy A, Mengel M, Haas M. Thirty years of the International Banff Classification for Allograft Pathology: The past, present, and future of kidney transplant diagnostics. *Kidney Int*. 2022;101:678–691. https://doi.org/10.1016/j.kint.2021.11.028
18. Villarreal JZ, Pérez-Anker J, Puig S, et al. *Ex vivo* confocal microscopy detects basic patterns of acute and chronic lesions using fresh kidney samples. *Clin Kidney J*. 2023;16:1005–1013. https://doi.org/10.1093/ckj/sfad019
19. Luciano RL, Moeckel GW. Update on the native kidney biopsy: Core curriculum 2019. *Am J Kidney Dis*. 2019;73:404–415. https://doi.org/10.1053/j.ajkd.2018.10.011